The hypersaline synthesis of titania: from powders to aerogels

UNIVERSITÀ DEGLI STUDI DI TORINO

The hypersaline synthesis of titania: from powders to aerogels

Roberto Nisticò[a,]*, Giuliana Magnacca[a]

[a] University of Torino, Department of Chemistry and NIS Research Centre, Via P. Giuria 7, 10125 Torino, Italy
* Corresponding author. E-mail: roberto.nistico@unito.it; Fax: +39-011-6707855; Tel: +39-011-6707533.

Abstract

High surface area mesoporous titania has been synthesized using ordinary salts (chlorides) for morphology control during the sol–gel process. Applying Ti-alkoxide (TTIP) as a titania precursor and a highly concentrated hypersaline medium, different results have been obtained according to the dispersing medium selected. By working in an acid environment, the hypersaline medium controls the oxide network growth, since different salts (and different salts amount) influence the surface area, porosity, crystallinity and polymorphs rearrangement of the final material, favoring the formation of acicular-like rutile at mild conditions. Nevertheless, it has been verified that, according to the Hofmeister series, salting-in ions induce an increase in the titania surface area, going from 79 (for the reference, without any salts) up to 253 $m^2 g^{-1}$ (for the Li-templated titania). By working in alcoholic media, the hypersaline environment favors the gelification process and the formation of amorphous titania aerogels or highly porous monoliths, according to the drying conditions selected (respectively supercritical CO_2 or ambient pressure air drying). Two different alcoholic media (ethanol and 2-propanol) have been compared. Such salt-templated titania aerogels are mesoporous (with BET surface area comprised between 322 and 490 $m^2 g^{-1}$). Besides the surface area, even the pore volume and the pore size can be controlled by both the reaction medium and the drying step: in particular, air-dried monoliths are small mesoporous (BET surface area between 419 and 518 $m^2 g^{-1}$). Reference materials synthesized in alcoholic media without using any salts do not gelify (thus confirming the importance of the hypersaline medium), whereas titania particles precipitate, inducing aggregation into small mesoporous powders. In general, the hypersaline-mediated titania production seems to be an interesting chemical toolbox, sustainable, highly efficient and also potentially suitable for industrial scaling-up.

1. Introduction

Titanium dioxide (TiO_2) is an important photo-catalytic material that in nature exists in three different polymorph crystallographic phases: the stable rutile and the two metastable anatase and brookite.[1,2] All the forms of titania have been applied in many technological fields, including energetic and environmentally friendly applications (for instance lithium batteries, solar cells, photo-catalytic devices for water photo-splitting as well as for the treatment of polluted air or water).[4–8]

Rutile, the most commonly diffuse polymorph species of titanium dioxide, presents a body-centred tetragonal unit cell and, therefore, its crystals usually appear as elongated acicular or prismatic structures.[1,3,9]

Even though it is well established that rutile is the most thermodynamically stable form of titanium dioxide, anatase remains the most kinetically favoured one, whereas brookite (the other orthorhombic titania polymorph) is difficult tosynthesize and thus shortly investigated.[10] According to this, anatase is usually the most easy-obtainable crystalline specie of TiO_2 at mild conditions, whereas it can be simply converted into the thermodynamically stable rutile form just by heating at temperatures between 400 °C to 1200 °C, through a time dependent reconstructive transition (which involves breaking and formation of chemical bonds)[11,12] according to processing methods available in the literature.[1,13] Although the most diffuse method for obtaining rutile phase is through high temperature thermal treatments of titania specimens, it is also possible to form rutile under mild conditions, almost close to Room Temperature (RT in the following), by hydrothermal synthesis with a controlled precipitation of rutile crystals from the liquid phase.[1,2,14–17] Moreover, the

formation of pure rutile nanocrystals is promoted by hydrolysis of Ti(IV) under acidic condition in the presence of highly concentrated chloride medium.[18–20] In this condition Ti(IV) ions organize in octahedral coordination by forming several complexes with the ligands present in the hydrothermal system (i.e. H_2O, OH^- and Cl^-) and oligomerize in dimers and trimers possessing a structural unit similar to the rutile crystal lattice.[20]

Therefore, at least in principle, it should be possible to obtain titania in rutile phase using a recently presented method for the production of micro and mesoporous carbons[21,22] and mesoporous silicas[23] under hypersaline conditions in the procedure called "salt-templating". In this particular procedure, concentrated solutions (or even melts) of ordinary inorganic salts are mixed with a material precursor which is condensed and scaffolded in the presence of the salts. The obtained materials possess high surface area and pore shape corresponding to the molecules, salt clusters and their percolation structures. The pores formation in hypersaline systems is controlled by the ability of the salts to stabilize the colloidal system forming fractal structures or networks (salting-in effect) or to induce particles formation (salting-out effect), according to the Hofmeister series.[24–26] Salts are then easily removed by simple washing with water. This procedure was proven also to allow the production of aerogels stable enough to be dried without employing supercritical CO_2.[22,27]

The production of titania in form of aerogel is an actual challenge because it is possible to obtain materials porous andwith high surface area but often this causes the lack of supercritical drying procedure simplicity. As reported in the literature by Husing et al.,[28] titania aerogels can be prepared totally amorphous or made of a network of anatase particles. Amorphous titania aerogels, obtained after high temperature supercritical drying, show ca. 170 $m^2\ g^{-1}$ of BET surface area and pore volume of 0.50 $cm^3\ g^{-1}$, whereas anatase aerogels (obtained after calcination of the amorphous phase) present a surface area of ca. 100 $m^2\ g^{-1}$.[29] Campbell et al.[30] registered the formation of anatase/amorphous titania aerogels after low temperature supercritical drying with BET surface area in the range 600–700 $m^2\ g^{-1}$, but this result was obtained applying a tedious semi-continuous extraction of supercritical CO_2.

Additionally, titania aerogels are known for their mechanical fragility,[31] therefore crack-free titania aerogels are often composite materials because they need to be fabricated by adding in the formulation silica sol, acting as a nanoglue.[29,31]

To overcome these issues we propose the use of salt templating procedure which has been used with good results for the production of silica aerogels.[27] In this case titania samples have been synthesized by using TTIP (Titanium(IV)-Tetra-Iso-Propoxide) as titania precursor in the presence of different metal chlorides. In particular, the production of titania rutile powders at mild conditions has been investigated by using simple monovalent chlorides aqueous solutions as hypersaline medium. Moreover, TiO_2 aerogels (prepared applying a supercritical CO_2 drying step) and/or monoliths (considering a simple drying at ambient pressure) using $ZnCl_2$ as hypersaline medium and ethanol or 2-propanol as alcoholic environments was studied and compared with the classical TiO_2 aerogels synthesis, highlighting the effect due to the gel aging step. The choice of $ZnCl_2$ derived from the attempts to prepare aerogels using monovalent and bivalent chlorides. Monovalent species (for instance KCl, NaCl and LiCl) are not soluble or poorly soluble in alcoholic media, resulting not suitable for the production of aerogels. Among bivalent species, $ZnCl_2$, already used for the preparation of SiO_2 aerogels with good results, allowed to synthesized TiO_2 aerogels (and also monoliths) with valuable behaviors. Also $MgCl_2$ and $CaCl_2$ were considered but they gave problems in the removal of salts after the alcogels aging, therefore they were excluded from the present study.

2. Experimental

2.1 Materials

Titanium(IV)-Tetra-Iso-Propoxide (TTIP, CAS 546-68-9, assay = 97%, Aldrich) was selected as titania precursor. Inorganic salts selected were: sodium chloride (NaCl, CAS 7647-14-5, assay ≥99%, Sigma), potassium chloride (KCl, CAS 7447-40-7, assay ≥99.5%, Sigma Aldrich), lithium

chloride (LiCl, CAS 7447-41-8, assay ≥98%, Fluka) and zinc chloride ($ZnCl_2$, CAS 7646-85-7, assay ≥97%, Sigma Aldrich). Hydrochloric acid 1 M solution (HCl, CAS 7647-01-0, Merck) was used as acid catalyst for the synthesis of titania powders, whereas absolute ethanol (CAS 64-17-5, assay ≥99.8%, Sigma Aldrich) and 2-propanol (CAS 67-63-0, assay = 99.9%, VWR International) were used as alcoholic solvents for the aerogels and porous monoliths synthesis. All chemicals were used without purification.

2.2 Salt-templating synthesis of titania powders

A modification of the salt-templating procedure conducted in hypersaline aqueous medium for the synthesis of mesoporous silica powders was employed.[23] Inorganic salts were firstly dissolved at RT in 1 M HCl (15 ml) and then mixed with the titania precursor TTIP (1 g). The resulting mixtures were placed into a glass vial and put into an oil bath at 50 °C for 10 days under magnetic stirring. Afterwards, samples were heated into an oven at 60 °C for several hours. In order to remove the residual porogen salts, materials were grinded and washed twice in water for several hours and finally filtered and dried at 60 °C in vacuo. Different amounts of sodium chloride were added to the mixture (0.5, 1, 2 and 3 g) in order to evaluate the effect of the porogen amount, whereas potassium chloride and lithium chloride were only added in amount of 2 g to evaluate the effect of the salt cation. A reference material was also prepared in the same way just leaving out the salt in order to evidence the porogen action. Samples were named SaTi-X-Y, where SaTi stands for Salt/Titania, X for the type of cation of the templating salt (namely Na^+, K^+, Li^+ and 0 for the reference) and Y for the salt/TTIP mass ratio used in the synthesis.

2.3 Salt-templating synthesis of titania aerogels and monoliths

A modification of the salt-templating procedure conducted in hypersaline alcoholic medium for the synthesis of mesoporous silica aerogels/porous glasses was employed.27 2 g of inorganic salt ($ZnCl_2$) were dissolved in 8ml of ethanol (or 2-propanol), and 2 g of TTIP were added afterwards. In particular, zinc chloride was used as inorganic salts. After few hours of stirring in order to homogenize the mixture, the solution was left in air at RT in an open glass vial. Alcogels formed were extracted from the vials after different times (7, 10 and 15 days), and submitted to a dialysis process to remove inorganic templates and byproducts. The washing was carried out firstly in demineralized water (in order to remove the inorganic salts) and then in ethanol (in order to restore the initial alcoholic medium).

Afterwards, alcogels were dried, either in supercritical CO_2 or in air at ambient pressure, and physico-chemically characterized.

CO_2 supercritical dried materials were obtained by using a Bal-Tec CPD 030 Critical Point Dryer. Liquid carbon dioxide was flushed inside the autoclave chamber, covering completely the alcogels. After 5 minutes the autoclave valve was opened and the fluid level was reduced. Samples were washed this way for 5 times in order to eliminate ethanol and fill the porosity of the sample with supercritical liquid CO_2 inside the closed chamber. After the last admission of CO2 in the closed vessel, the temperature was increased above the CO_2 critical point (31.1 °C and 73.8 bar). At around 40 °C and 90 bar, supercritical conditions were reached and CO_2 turned into a gas phase.

During a slow depressurization, air progressively filled the porosity of the material, generating the titania aerogel. Reference solutions (containing only TTIP and ethanol or 2-propanol, without any salts) were also prepared: the sol did not gelify and titania started to precipitate forming a white powder. Samples were named PT-W-X-Y-Z, where PT stands for Porous Titania, W indicates the selected cation (i.e. Zn^{2+} or 0 for the reference), X indicates the solvents (E for ethanol and P for 2-propanol), Y corresponds to the drying conditions (namely Sd for the Supercritical drying and Ad for the RT ambient pressure Air drying) and Z is the aging time (7, 10 or 15 days).

2.4 Characterization

Wide angle X-rays scattering (WAXS) patterns were measured on a Bruker D8 Advance instrument using Cu-Ka-radiation.
TEM micrographs were obtained using a Zeiss EM 912 Ω instrument at an accelerator voltage of 120 kV.
High Resolution Transmission Electron Microscopy (HRTEM) micrographs and Selected Area Electron Diffraction patterns (SAED) were obtained by using a JEOL 3010 instrument (300 kV) equipped with a LaB_6 filament.
SEM images were obtained on a LEO 1550-Gemini instrument after sputtering with platinum.
Nitrogen sorption measurements were carried out with N_2 at 77 K after outgassing the samples at 150 °C under vacuum for 20 hours using a Quantachrome Quadrasorb SI porosimeter. The specific surface area was calculated by applying the Brunauer–Emmett–Teller (BET) model[32] to the isotherm data points of the adsorption branch in the relative pressure range $0.06 < P/P_0 < 0.3$. The pore size distribution was calculated from N_2 sorption data using the Non-Local Density Functional Theory (NLDFT) model[33,34] for cylindrical pores provided by Quantachrome data reduction software QuadraWin Version 5.11.

3. Results and discussion

3.1 Salt-templated titania powders obtained in hypersaline conditions

For the synthesis of mesoporous titania powders by salt-templating approach, TTIP was selected as titania precursor. The reaction was conducted in acidic medium (1 M HCl) in order to moderate the polycondensation process. Sodium chloride was chosen as representative porogen salt and thoroughly analyzed in various experiments. In order to study the generality of the approach as well as the effect of different salts in the final structure, lithium chloride and potassium chloride were also investigated under fixed conditions.
After dissolution of the salts in acid solution and addition of TTIP, polycondensation reactions were conducted by heating at 50 °C. During this process, the titania network is formed in the presence of the inorganic salts and obtained either as a white particulate solid in case of templating with salting-out ions (Na^+ and K^+) or as a light pink-whitish substance in case of templating with salting-in ions (Li^+).
The morphologic appearance of the reference sample synthesized without any salt (SaTi-0-0) and in the presence of salts highlights the differences between the obtained materials. With respect to the reference (Fig. 1A and D), samples SaTi-Na-2 (Fig. 1B and E) and SaTi-Li-2 (Fig. 1C and F) appear less dense. Moreover, Na and K-templated materials (the images of the latter are reported in Fig. S1D and S1H, ESI) are made by acicular particles of rutile phase (confirmed by HRTEM image reported in Fig. 2) whereas the Li-templated one is made by a tridimensional network, as expected considering the salting-out and salting-in effects of the three cations selected. Also the reference material seems to be made by acicular particles, but shorter, thicker and characterized by an important aggregation if compared to SaTi-Na-2 and SaTi-K-2 samples. Finally, the increase of NaCl amount in the SaTi-Na-Y series brings an increase in softness and fluffiness of the final material, although the microscopic aspect does not change very much.
Wide angle X-ray scattering patterns of all the products (obtained after washing) are reported in Fig. S2, ESI. The typical diffraction pattern of rutile, with intense signals corresponding to (110), (101), (111) and (211) planes,[35,36] is revealed in all the diffractograms. The absence of additional peaks indicates the effective removal of the inorganic salt species by washing. The rutile phase has been detected also in the reference material, whereas the LiCl material presents a shoulder at $2\theta = 25°$ and a scarcely detectable signal at $2\theta \sim 48°$, that might correspond to the (101) and (200) anatase planes, respectively.[36]
The crystalline structure of the materials obtained with this method appears quite odd, since only in one case it is possible to detect a small amount of the most common anatase phase, whereas rutile is present in all the systems.

Actually, together with the presence of chloride groups which induce the organization of octahedral Ti(IV) complexes in rutile arrangement, as discussed above,[1,18–20] also the acidity of the reaction media plays a very important role in the crystalline phase formation.[35]
In fact, lower the pH, lower the kinetic of the titanium alkoxide hydrolysis and therefore easier the organization of the network in crystal domains which can be builted up by condensation of TiO_6 octahedral systems through face-sharing or edge-share linking, favoring anatase or rutile phases, respectively.[19,37] In this discussion, the effect of the cations on the crystal arrangement cannot be explained but it is not possible to exclude some peculiar action bonded to their salting-in/salting-out effect. In fact, LiCl, the only representative of the salting-in group analyzed, seems to induce, together with the rutile formation, the growth of a small amount of anatase phase.
Nitrogen sorption measurements were performed on reference and templated samples, and the results are reported in Table 1 and Fig. 3. All the isotherms show a profile IV (according to the IUPAC classification) with hysteresis loops poorly visible, except for the LiCl-templated system (salting-in effect), which results, as for TEM analyses, different from NaCl and KCl-templated samples (salting-out effect). In all cases, the salt addition results in an increased nitrogen uptake compared to the reference material. BET surface areas significantly increase starting from 79 $m^2 g^{-1}$ for the reference material, ranging from 93 $m^2 g^{-1}$ up to 111 $m^2 g^{-1}$ for the NaCl-templated series, arriving to 114 for KCl-templated sample and 253 $m^2 g^{-1}$ for the LiCl-templated one. Analogously, the DFT total porosity increases starting from 0.11 $cm^3 g^{-1}$ for the reference material, ranging from 0.14 to 0.18–0.19 $cm^3 g^{-1}$ for the NaCl-templated series, arriving to 0.19 $cm^3 g^{-1}$ for KCl-templated sample and 0.27 $cm^3 g^{-1}$ for the LiCl-templated one.
The pore size distribution relative to reference material indicates the presence of mesoporosity of ca. 60 Å of width. In the NaCl series (Fig. 3, top), NaCl addition in amount of 0.5 g causes the decrease of the 60 Å pores and the contemporary formation of a new family of small mesopores of ca. 30 Å of width which is also visible for the 1 g NaCl-templated sample. For further addition of porogen, the small mesoporosity disappears, the pores of ca. 60 Å of width increases again and a new class of larger and less defined pores appears and continues increasing with the NaCl amount.
The influence of the salt nature on the pore size distribution is described in Fig. 3, bottom right section. The curves indicate the presence of pores of ca. 60 Å of width and the formation of larger porosity in the presence of Na^+ and K^+ cations. Li^+ cation, instead, modifies the trend causing a strong increase of the 60 Å pores with a very small contribution given by the larger pores.
Considering the data above discussed, also titania synthesis, as well as silica preparation, is affected by salting-in/salting-out effect of inorganic salts, since they promote a system-demixing (salting-out cations, i.e. Na^+ and K^+) or a network formation (salting-in cations, i.e. Li^+). In the first case a broader pore distribution has been obtained, given by particle aggregation, whereas in the latter case a more homogeneous system with higher pores volume and a more defined pore size distribution has been formed. In general, it has been confirmed that ions rich environments (hypersaline medium) influence the titania network growth and different salts (and different salt amounts) can influence not only the surface area and the porosity of the final materials, but also the polymorphs rearrangement.

3.2 Salt-templated titania aerogels and other porous systems obtained in hypersaline conditions

For the synthesis of titania aerogels and/or porous monoliths by the salt-templating approach, TTIP was selected as titania precursor and the reaction was conducted in alcoholic media (ethanol or 2-propanol) since alcohols promote aerogels formation and guarantee a fast evaporation.[38] Zinc chloride was chosen as inorganic salts constituting the hypersaline medium (in analogy with our previous study concerning the production of silica aerogels).[27] The hypersaline medium should modify the sol–gel procedure since dissolved ions work also as catalysts for the polycondensation reactions for the oxide network formation. After dissolution of the salts in the alcoholic medium and

addition of TTIP, polycondensation reactions take place and gelification occurs giving opaque-transparent or milky-white alcogels depending on the selected solvent, i.e. ethanol and 2-propanol respectively.
No gelification occurs preparing the reference solutions, containing only TTIP and ethanol or 2-propanol without any salts. This behavior suggests that the hypersaline medium drives the formation of aerogels or monoliths, whereas the absence of salts induces the formation of very fragile structures generated by particles aggregation.
An overview of titania aerogels and porous monoliths prepared in the two solvents environment and after 7, 10 and 15 days of gel aging time is reported in the ESI (see Figures from S3 to S6).
All the Zn-templated samples obtained in ethanol via CO_2 supercritical drying are transparent, whereas air-dried materials obtained in ethanol are yellowish. Vice versa, materials obtained in 2-propanol, independently from the drying method, appear milky-white.
Unexpectedly, salt-templated monoliths are rather compact and stable whereas it is known that pure titania aerogels are difficult to obtain, since they tend to collapse (usually silica sol is added to the synthesis mixture).[29,31] Conversely, salt-templated monoliths present good mechanical properties without using additives.
WAXS patterns (Fig. S7, ESI) indicate that both reference and Zn-templated air-dried titania are mainly amorphous, whereas Zn-templated supercritically dried samples present a small amount of anatase phase (main signal at $2\theta = 25°$).
This suggests that the supercritically drying allows an organization, although limited, of titania in crystalline form which is not achieved by air-dried and reference titania samples.
BET surface area and porosity data of all samples are reported in Table 2, whereas N_2 adsorption measurements and pore sizes distribution of Zn-templated titania samples are reported in Fig. 4 (for the ones obtained in ethanol medium) and Fig. 5 (for the ones obtained in 2-propanol medium). Analogously, reference materials curves are reported in the ESI section.
In general, all titania isotherms are of type IV (according to the IUPAC classification). In particular, the isotherms of CO_2 supercritical dried Zn-templated materials are characterized by having an hysteresis loop of H2 type in the relative pressure range of 0.6–1, typical for medium-large mesoporous systems, whereas the trend for the air-dried Zn-templated materials is typical for small mesoporous systems.
BET surface area values relative to supercritically dried Zn-templated samples are in the range of 320–490 $m^2\ g^{-1}$ with pore volume of 0.49–1.25 $cm^3\ g^{-1}$. Such data are close to those typical for titania aerogels obtained by classical synthetic processes,[28,39] but without using silica as additive. Almost different is the trend registered for the air-dried Zn-templated materials, since BET surface area values are still in the range of 419–518 $m^2\ g^{-1}$ but pore volume decreases to 0.23–0.31 $cm^3\ g^{-1}$, thus probably indicating a limited collapse of the structure.
The DFT pore size distribution curves allow to examine the porosity of the obtained materials. Zn-templated supercritically dried samples obtained in ethanol environment (Fig. 4, top) show a bimodal DFT pore size distribution centered at 40 and 120 Å of pore width, which moves to 40–80 Å increasing the aging time. By changing the alcoholic medium to 2-propanol (Fig. 5, top), porosity becomes less ordered and increases in size reaching the macropore range.
Air-dried samples produced in both alcoholic media (Fig. 4 and 5, bottom) present a sharp pore size distribution centered at 40 Å of width, however no trends induced by aging time are revealed.
Conversely, reference materials synthesized without using any templating agents show BET surface area comprised between 298 and 778 $m^2\ g^{-1}$ with total pore volume between 0.15 and 0.49 $cm^3\ g^{-1}$. All samples have a DFT pore size distribution centered at 30–40 Å of pore width, whereas air-dried ones have a shoulder at larger width values (Fig. S8 and S9, ESI). The aging effect is much more visible for air-dried materials with respect to supercritically dried ones, since the porosity decreases by increasing the gel aging time.
Basing on these results, it has been possible to conclude that supercritically dried materials template in the presence of $ZnCl_2$ hypersaline medium are highly porous aerogels, whose porosity can be

modulated by changing both the alcoholic medium and the aging time. In particular, the use of 2-propanol as solvent induces the formation of larger pores if compared to the ethanol, whereas the increase of the aging time causes the change of the pores volume.
Surprisingly, air drying process can substitute the more complex supercritical drying when dealing with salt-templated TiO_2, since it allows to obtain a good and stable mesoporosity in the system. Moreover, since stable monoliths were obtained without using silica, it has been confirmed the important role of inorganic salts as stabilizing agents in the sol–gel process for the synthesis of pure titania aerogels materials.

4. Conclusions

The effect of hypersaline medium in the synthesis of titania (both powders, and aerogels and monoliths) was here presented. Materials were synthesized from TTIP as titania precursor and ordinary chlorides aqueous solutions were used at high concentrations as hypersaline media.
Concerning the powdery systems, a facile and efficient one-pot method for the production of titania nanoparticles was here presented. It has been verified that the hypersaline medium influences the titania network growth, whereas the nature and composition of the ions-rich medium can influence the surface area, porosity and polymorphs rearrangement in the final material, favouring the rutile acicular structure (in particular for salting-out cations), even at mild conditions. Moreover, salts can be easily removed just by water-washing, thus enabling the production of samples without using special equipment or safety concerns. The basis of this synthetic route can be explained by means of the Hofmeister series. In fact, just by changing the amount of the salts and/or the type of cation, going from Na^+ and K^+ (salting-out ions) to Li^+ (more salting-in ion), it was possible to control the morphology of the final material. Furthermore, it has been verified that salting-in ions induce an increase of the surface area and porosity of the final material (analogously to what already verified for silica systems).
Concerning the aerogels production, the synthesis conducted in a $ZnCl_2$-rich alcoholic medium (ethanol or 2- propanol) allowed the formation of titania aerogels or highly porous monoliths, according to the drying conditions selected (supercritical or air-drying, respectively). Results indicate that:

i. Zn-templated samples are amorphous (whereas the supercritical dried ones present a slightly amount of anatase).
ii. Zn-templated supercritical dried samples are mesoporous, whereas the air dried ones are mostly small mesoporous.
iii. Zn-templated samples synthesized in ethanol are transparent, whereas the ones obtained in 2-propanol are milky-white (coarser structure), implying different optical properties.

Although pure titania aerogels are in general difficult to be obtained, since the titania network is weak and tends to collapse, the aerogels and porous monoliths obtained via hypersaline synthesis are rather stable.
In conclusion, since both the processes here proposed for the production of titania materials (in form of powders or aerogels/monoliths) are carried out at relatively low temperatures and since the species forming the hypersaline media can be easily removed (by simple water-washing) and in principle recovered afterwards, the entire approach here proposed is not only sustainable, but also potentially suitable for the industrial production.

5. Acknowledgements

This work was supported by the Max Planck Society and University of Torino. Compagnia di San Paolo and University of Torino are gratefully acknowledged for funding Project ORTO114XNH. The authors thank Prof. M. Antonietti and Dr N. Fechler (from Max Planck Institute of Colloids and Interfaces, Potsdam-Golm, Germany) for the helpful teachings and the instrumentation availability, Dr G. Clavel (from Max Planck Institute of Colloids and Interfaces, Potsdam-Golm, Germany) for HRTEM measurements, Mr A. Vizintin (from National Institute of Chemistry, Ljubljana, Slovenia)

for aerogels and porous monoliths pictures and Mr V. Molinari (from Max-Planck Institute of Colloids and Interfaces, Potsdam-Golm, Germany) for the very precious help.

References and notes

1 D. A. H. Hanaor and C. C. Sorrell, J. Mater. Sci., 2011, 46, 855.
2 G. Li, L. Li, J. Boerio-Goates and B. F. Woodfield, J. Mater. Res., 2003, 18, 2664.
3 O. Carp, C. L. Huisman and A. Reller, Prog. Solid State Chem., 2004, 32, 33.
4 D. Vione, C. Minero, V. Maurino, M. E. Carlotti, T. Picatonotto and E. Pelizzetti, Appl. Catal., B, 2005, 58, 79.
5 A. Fujishima, T. N. Rao and D. A. Tryk, J. Photochem. Photobiol., C, 2000, 1, 1.
6 A. Fujishima, X. Zhang and D. A. Tryk, Surf. Sci. Rep., 2008, 63, 515.
7 B. E. Hardin, A. Sellinger, T. Moehl, R. Humphry-Baker, J.-E. Moser, P. Wang, S. M. Zekeeruddin, M. Gr¨atzel and M. D. McGehee, J. Am. Chem. Soc., 2011, 133, 10662.
8 L. Kavan, M. Kalbac, M. Zukalova, I. Exnar, V. Lorenzen, R. Nesper and M. Gr¨atzel, Chem. Mater., 2004, 16, 477.
9 J. Moellmann, S. Ehrlich, R. Tonner and S. Grimme, J. Phys.: Condens. Matter, 2012, 24, 424206.
10 A. Beltran, L. Gracia and J. Andres, J. Phys. Chem. B, 2006, 110, 23417.
11 R. L. Penn and J. F. Banfield, Am. Mineral., 1999, 84, 871.
12 G. H. Lee and J.-M. Zuo, J. Am. Ceram. Soc., 2004, 87, 473.
13 J. Sun, L. Gao and Q. Zhang, J. Am. Ceram. Soc., 2003, 86, 1677.
14 R. R. Bacsa and J. Kiwi, Appl. Catal., B, 1998, 16, 19.
15 H. Shin, H. S. Jung, K. S. Hong and J.-K. Lee, J. Solid State Chem., 2005, 178, 15.
16 C. C. Wang and J. Y. Ying, Chem. Mater., 1999, 11, 3113.
17 G. Li, J. Boerio-Goates, B. F. Woodfield and L. Li, Appl. Phys. Lett., 2004, 85, 2059.
18 L. Ciavatta, D. Ferri and G. Riccio, Polyhedron, 1985, 4, 15.
19 H. Cheng, J. Ma, Z. Zhao and L. Qi, Chem. Mater., 1995, 7, 663.
20 V. D. Hildenbrand, H. Fuess, G. Pfaff and P. Reynders, Z. Physiol. Chem., 1996, 194, 139.
21 N. Fechler, T.-P. Fellinger and M. Antonietti, Adv. Mater., 2013, 25, 75.
22 N. Fechler, S.-A. Wohlgemuth, P. Jaker and M. Antonietti, J. Mater. Chem. A, 2013, 1, 9418.
23 R. Nisticò, G. Magnacca, M. Antonietti and N. Fechler, Z. Anorg. Allg. Chem., 2014, 640, 582.
24 N. Schwierz, D. Horinek and R. R. Netz, Langmuir, 2013, 29, 2602.
25 E. Leontidis, Curr. Opin. Colloid Interface Sci., 2002, 7, 81.
26 M. G. Cacace, E. M. Landau and J. J. Ramsden, Q. Rev. Biophys., 1997, 3, 241.
27 R. Nisticò, G. Magnacca, M. Antonietti and N. Fechler, Adv. Porous Mater., 2014, 2, 37.
28 N. Husing and U. Schubert, Angew. Chem., Int. Ed., 1998, 37, 22.
29 M. Schneider and A. Baiker, Catal. Today, 1997, 35, 339.
30 L. K. Campbell, B. K. Na and E. I. Ko, Chem. Mater., 1992, 4, 1329.
31 C. A. Morris, M. L. Anderson, R. M. Stroud, C. I. Merzbacher and D. R. Rolison, Science, 1999, 284, 622.
32 S. Brunauer, P. H. Emmett and E. Teller, J. Am. Chem. Soc., 1938, 60, 309.
33 D. L. Ou, P. D. Chevalier, I. A. Mackinnon, K. Eguchi, R. Boisvert and K. Su, J. Sol-Gel Sci. Technol., 2003, 26, 407.
34 R. Nisticò, D. Scalarone and G. Magnacca, Microporous Mesoporous Mater., 2014, 190, 208.
35 D. Zang, L. Qi, J. Ma and H. Cheng, J. Mater. Chem., 2002, 12, 3677.
36 J. Yan, G. Wu, N. Guan, L. Li, Z. Li and X. Cao, Phys. Chem. Chem. Phys., 2013, 15, 10978.
37 J. Rubio, J. L. Oteo, M. Villegas and P. Duran, J. Mater. Sci., 1997, 32, 643.
38 M. Moner-Girona, A. Roig and E. Molins, J. Sol-Gel Sci. Technol., 2003, 26, 645.
39 G. Dagan and M. Tomkiewicz, J. Non-Cryst. Solids, 1994, 175, 294.

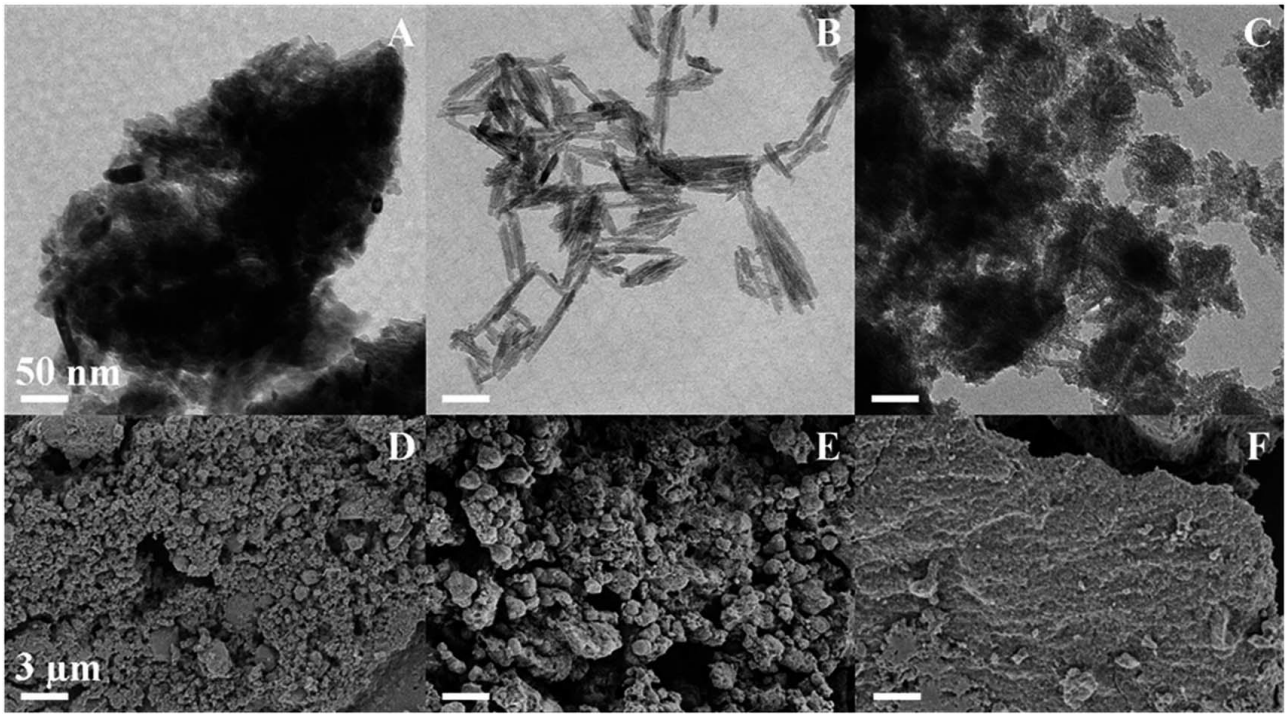

Figure 1. TEM (upper row) and SEM (lower row) images of salt-templated titania powders obtained by varying the salt nature. From left to right: salt-free reference SaTi-0-0 (A and D), NaCl-templated SaTi-Na-2 (B and E) and LiCl-templated SaTi-Li-2 (C and F).

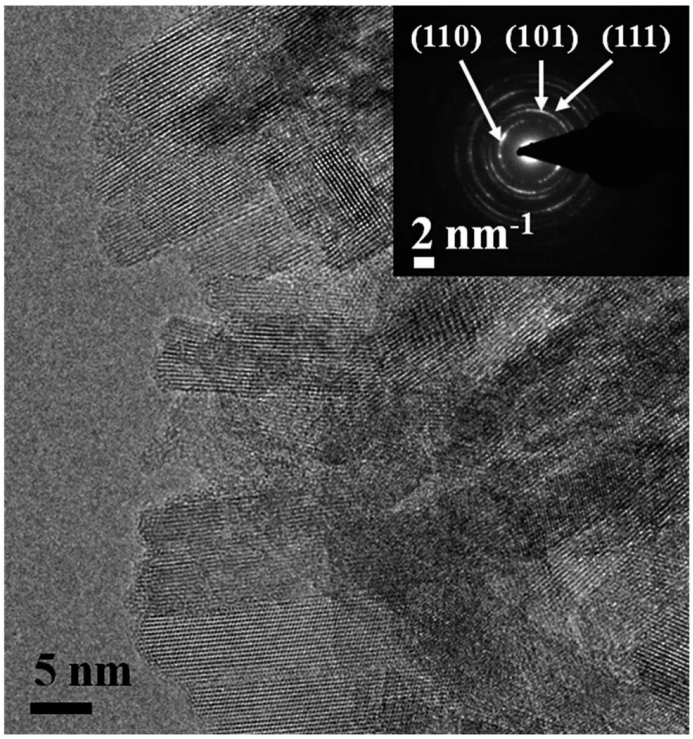

Figure 2. HR-TEM micrograph and SAED pattern (inset) of NaCl-templated SaTi-Na-2 powder, highlighting the rutile acicular crystalline structure.

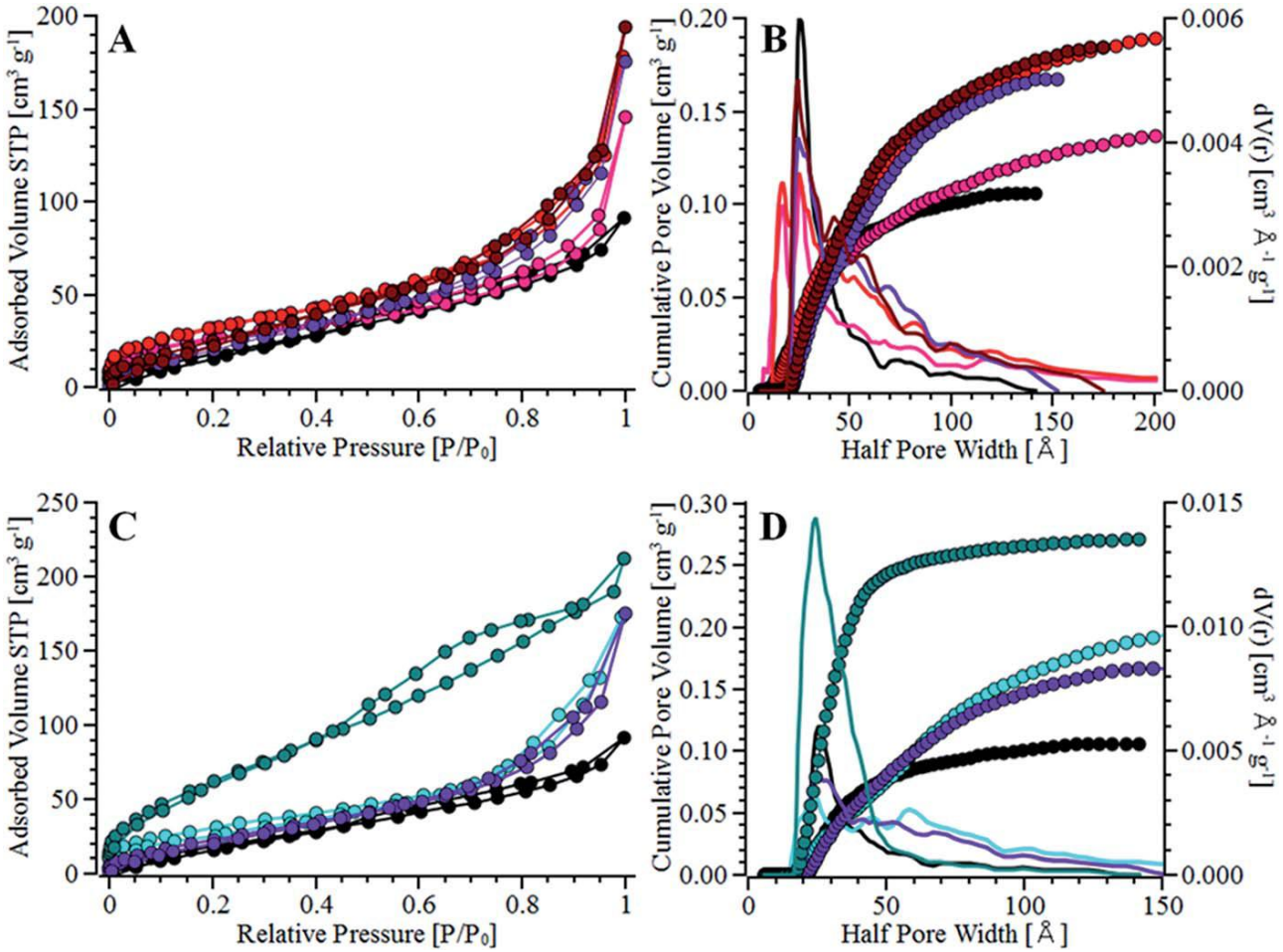

Figure 3. Nitrogen sorption isotherms (left) and pore size distribution (right) of salt-templated titania at varying amount (A and B) and nature (C and D) of the salt: SaTi-0-0 (black), SaTi-Na-0.5 (pink), SaTi-Na-1 (red), SaTi-Na-2 (violet), SaTi-Na-3 (brown), SaTi-K-2 (light cyan), SaTi-Li-2 (dark cyan).

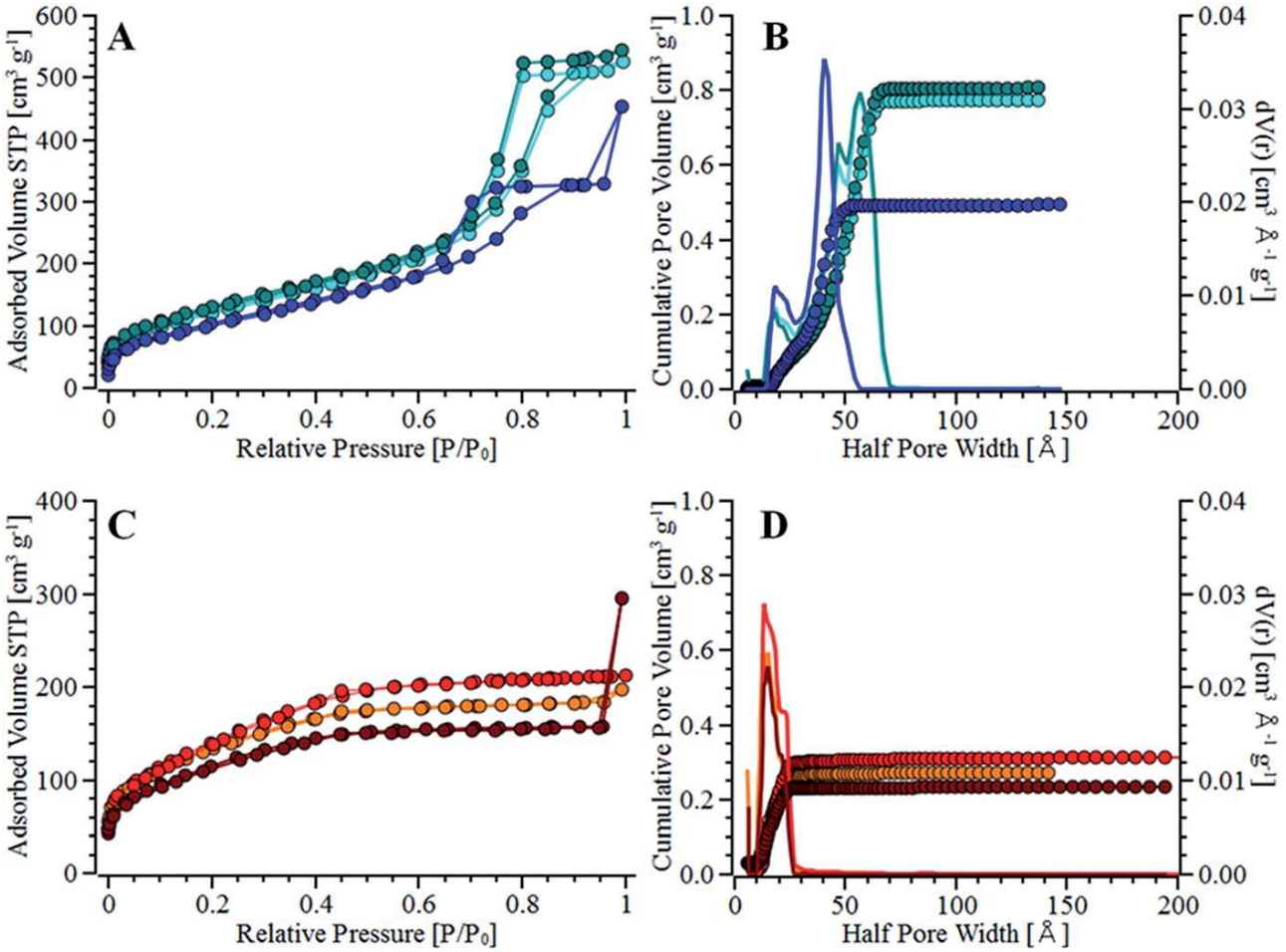

Figure 4. Nitrogen sorption isotherms (left) and pore size distribution (right) of Zn-templated titania obtained in ethanol CO_2 supercritical dried (A and B) and RT ambient pressure air dried (C and D) at varying aging time: PT-Zn-E-Sd-7 (light cyan), PT-Zn-E-Sd-10 (dark cyan), PT-Zn-E-Sd-15 (blue), PT-Zn-E-Ad-7 (orange), PT-Zn-E-Ad-10 (red), PT-Zn-E-Ad-15 (brown).

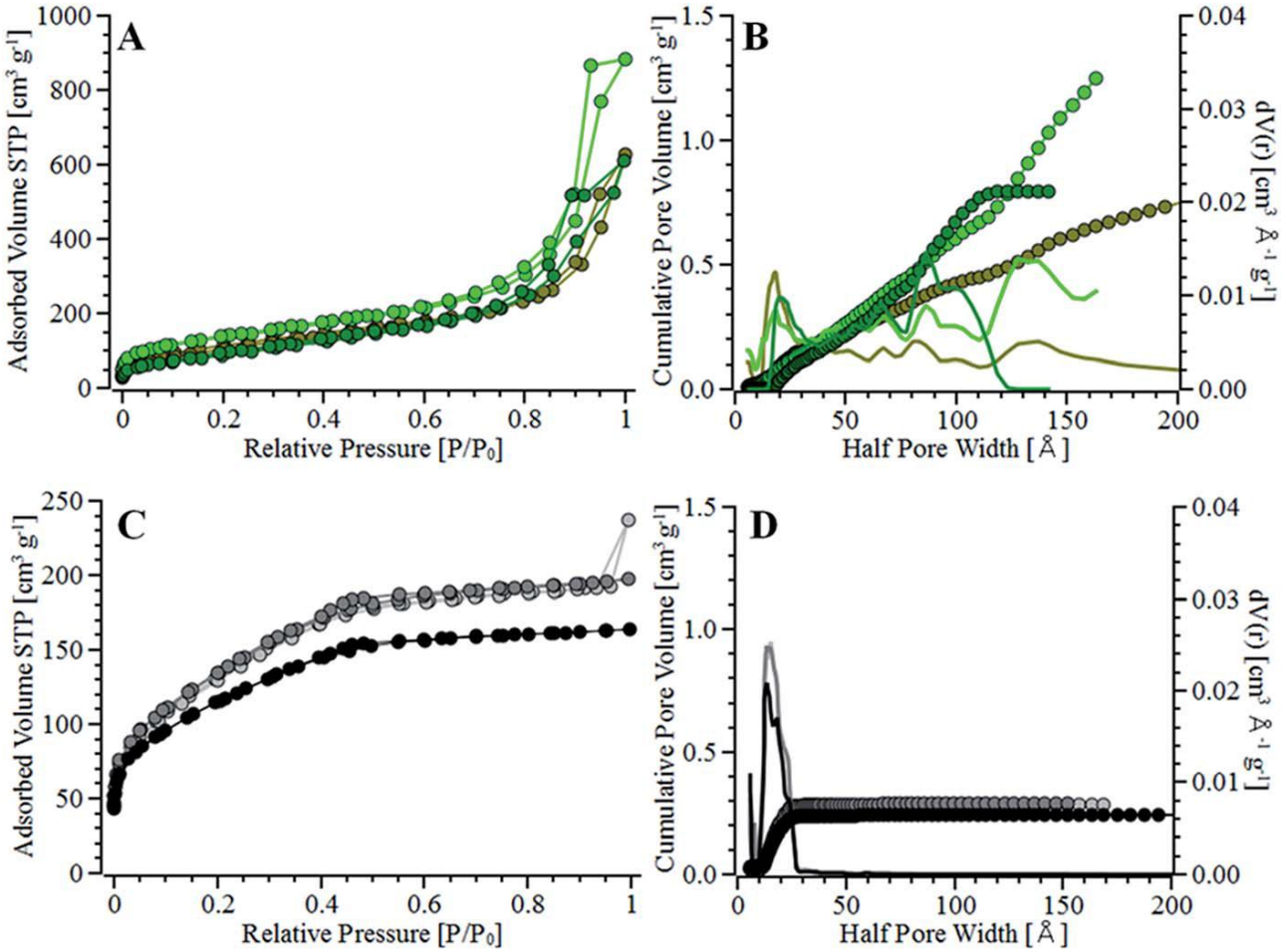

Figure 5. Nitrogen sorption isotherms (left) and pore size distribution (right) of Zn-templated titania obtained in 2-propanol CO_2 supercritical dried (A and B) and RT ambient pressure air dried (C and D) at varying aging time: PT-Zn-P-Sd-7 (dark yellow), PT-Zn-P-Sd-10 (light green), PT-Zn-PSd-15 (dark green), PT-Zn-P-Ad-7 (light grey), PT-Zn-P-Ad-10 (dark grey), PT-Zn-P-Ad-15 (black).

Table 1. BET surface areas and NLDFT total pore volumes relative to reference and templated powders.

Samples name	BET surface area [m^2 g^{-1}]	Pore volume [cm^3 g^{-1}]
SaTi-Na-0.5	93	0.14
SaTi-Na-1	118	0.19
SaTi-Na-2	102	0.17
SaTi-Na-3	111	0.18
SaTi-K-2	114	0.19
SaTi-Li-2	253	0.27
SaTi-0-0	79	0.11

Table 2. BET surface areas and NLDFT total pore volume of aerogels and highly-porous titania materials

Samples name	BET surface area [m^2 g^{-1}]	Pore volume [cm^3 g^{-1}]
PT-Zn-E-Sd-7	449	0.77
PT-Zn-E-Sd-10	482	0.81
PT-Zn-E-Sd-15	395	0.49
PT-Zn-E-Ad-7	487	0.27
PT-Zn-E-Ad-10	518	0.31
PT-Zn-E-Ad-15	424	0.23
PT-Zn-P-Sd-7	420	0.76
PT-Zn-P-Sd-10	490	1.25
PT-Zn-P-Sd-15	322	0.79
PT-Zn-P-Ad-7	470	0.28
PT-Zn-P-Ad-10	491	0.29
PT-Zn-P-Ad-15	419	0.24
PT-0-E-Sd-7	580	0.27
PT-0-E-Sd-10	514	0.28
PT-0-E-Sd-15	461	0.23
PT-0-E-Ad-7	778	0.49
PT-0-E-Ad-10	584	0.28
PT-0-E-Ad-15	298	0.15

PT-0-P-Sd-7	486	0.32
PT-0-P-Sd-10	506	0.30
PT-0-P-Sd-15	620	0.36
PT-0-P-Ad-7	519	0.35
PT-0-P-Ad-10	562	0.33
PT-0-P-Ad-15	441	0.22